ELSEVIER

Materials Science and Engineering B 136 (2007) 187–192

MATERIALS SCIENCE & ENGINEERING B

www.elsevier.com/locate/mseb

# Structural characterization of chemically deposited PbS thin films

F.A. Fernández-Lima [a,b,*], Y. González-Alfaro [c], E.M. Larramendi [c], H.D. Fonseca Filho [b], M.E.H. Maia da Costa [b], F.L. Freire Jr. [b], R. Prioli [b], R.R. de Avillez [d], E.F. da Silveira [c], O. Calzadilla [c], O. de Melo [c], E. Pedrero [c], E. Hernández [c]

[a] *Instituto Superior de Tecnologías y Ciencias Aplicadas Ave Salvador Allende esq. Luaces, s/n, AP 6163, CP 10600, Ciudad de La Habana, Cuba*

[b] *Departamento de Física, Pontifícia Universidade Católica do Rio do Janeiro, 22453-900 Rio de Janeiro, RJ, Brazil*

[c] *Facultad de Física-IMRE, Universidad de La Habana, Cuba*

[d] *Departamento de Ciência dos Materiais e Metalurgia, Pontifícia Universidade Católica do Rio do Janeiro, 22453-900 Rio de Janeiro, RJ, Brazil*

Received 27 March 2006; received in revised form 21 September 2006; accepted 30 September 2006

**Abstract**

Polycrystalline thin films of lead sulfide (PbS) grown using substrate colloidal coating chemical bath depositions were characterized by RBS, XPS, AFM and GIXRD techniques. The films were grown on glass substrates previously coated with PbS colloidal particles in a polyvinyl alcohol solution. The PbS films obtained with the inclusion of the polymer showed non-oxygen-containing organic contamination. All samples maintained the Pb:S 1:1 stoichiometry throughout the film. The amount of effective nucleation centers and the mean grain size have being controlled by the substrate colloidal coating. The analysis of the polycrystalline PbS films showed that a preferable (1 0 0) lattice plane orientation parallel to the substrate surface can be obtained using a substrate colloidal coating chemical bath deposition, and the orientation increases when a layer of colloid is initially dried on the substrate.



*Keywords:* Semiconductors; Thin films; Sulfides; Ion beam; Diffraction; Surface morphology

## 1. Introduction

Polycrystalline PbS thin films are currently attracting interest mainly due to their potential as infrared detector materials [1,2]. These films can be obtained by several methods [3,4], but chemical bath deposition (CBD) is mostly used due to its low cost and the quality of the obtained films. The manufacture of advanced electronic devices with desired physical properties requires the availability of semiconductors films with controllable compositions, grain sizes and orientations. Indeed, the photosensitivity of the PbS polycrystalline thin film has a strong dependence with their structural and morphological characteristics [1,5].

The use of organic modifications of inorganic surfaces to promote the formation of films from liquid media has been a recent trend in thin films deposition. More recently, organic self-assembled monolayers have been used to tailor the chemical characteristics of substrate surfaces [6–14]. Many methods have been developed to fabricate PbS nanoparticles in micelles [15], polymers [16], zeolites [17], and monolayer surfaces [18]. The oriented crystallization of nanoparticles has been observed in the growth of PbS nanocrystals mediated by surfactant-polymer templates [19–26]. The effect of surface structure on photosensitivity in PbS thin films grown using a substrate colloidal coating chemical bath deposition has been reported [5].

In this paper, we describe the influence of a colloidal coating of the substrate surface (PbS particles in a alcohol polyvinyl solution) on the growth of PbS polycrystalline thin films by chemical bath deposition (CBD), using Rutherford backscattering spectrometry (RBS) and X-ray photoelectron spectroscopy (XPS) for the analysis of the elemental composition, thickness and stoichiometry of the films. In addition, the topography and structure of the films were characterized by grazing incidence X-ray diffraction data (GIXRD) and atomic force microscopy (AFM).

* Corresponding author at: Departamento de Física, Pontifícia Universidade Católica do Rio do Janeiro, 22453-900 Rio de Janeiro, RJ, Brazil.
Tel.: +55 21 31141272; fax: +55 21 3114 1040.
*E-mail address:* lazaro@vdg.fis.puc-rio.br (F.L. Freire Jr.).

0921-5107/$ – see front matter © 2006 Elsevier B.V. All rights reserved.
doi:10.1016/j.mseb.2006.09.029

## 2. Experimental details

The samples were grown using a traditional method of chemical bath deposition; its characteristics have been described in detail elsewhere [5]. It involves a previous seeding of germs on a glass substrate from a seeding solution to form a very thin layer. Afterwards the substrate is introduced in the solution of growth, until the film attains the desired thickness or the reaction is completed. The seeding process regulates the concentration of germs initially formed, ensuring a homogeneous distribution and a good adherence between film and substrate.

Before the immersion of the glass substrates into the growth solution, they were mechanically cleaned with detergent and rinsed in bi-distilled water (A). After that, three types of substrate treating were adopted:

- (B) Introduced in a solution of polyvinyl alcohol (2 g/l) for 24 h.
- (C) Immersed for 24 h in a colloidal solution of 166 ml of polyvinyl alcohol (6.0 g/l), 4 ml of $H_2S$ and 19 ml of $Pb(NO_3)_2$ (66.2 g/l).
- (D) Immersed for 24 h in a colloid solution of 166 ml of polyvinyl alcohol (6.0 g/l), 4 ml of $H_2S$ and 19 ml of $Pb(NO_3)_2$ (66.2 g/l) and dried in air for 10 min.

Afterwards, the substrates are introduced immediately in the chemical bath for 50 min. An adequate composition of the growth solution is: 19 ml of $Pb(NO_3)_2$ solution (6.62 g in 100 ml of $H_2O$); 1 ml of thiourea solution (10 g thiourea + 1 g $Na_2SO_3$ in 100 ml $H_2O$); 13 ml of alkaline solution (7.5 g NaOH in 100 ml $H_2O$). The components were added in the mentioned order (a change may provide a different product at the end), to obtain a final dark solution. The variant C was used in a previous work as a seeding process in order to provide nucleation centers and improve the adherence between film and substrate [1,5].

The RBS analysis was carried out using the 4 MV Van de Graaff KN-4000 accelerator from High Voltage Engineering Corp. of the Physics Department of the Pontifical Catholic University of Rio do Janeiro, Brazil. The RBS measurements were performed with 2.0 MeV $^4He^+$ ion beam and a surface barrier detector with 18 keV FWHM positioned at an angle of 165° with respect to the incident beam. The RBS spectra were analyzed using the RUMP code [27].

The AFM images were obtained with a Multimode AFM controlled by a Nanoscope IIIa electronics (Veeco) operated in taping mode. The grain size and shape measurements were determined by applying the Watershed technique [28], together with a shape factor algorithm [29]. The shape factor, define as $SF = 4\pi A/P^2$, were $P$ is the perimeter of the grain and $A$ its area, was used to obtain information about the shape of a grain. The surface roughness values ($R_{ms}$) were also determined. For the AFM image analysis, the ImageJ v. 1.33d program [30] was used with a home developed code. The used method was corroborated with the analyses made using KS400 Carl ZeissVision 3.0 code. The roughness values $R_{ms}$ were obtained from the AFM images of 30 μm × 30 μm scans. In the case of the shape factor SF, the analyses corresponds to the 5 μm × 5 μm scans in order to minimize the error of the perimeter identification and to have a relative good statistic in the number of grains per image.

Grazing incident X-ray diffraction measurements (GIXRD) were performed in the PbS films using the Cu Kα radiation of a ω-diffractometer (Siemens model D5000). The detector was equipped with a Soller slit for thin films and a LiF monochromator.

The XPS spectra were obtained using a Mg Kα X-ray source and a hemispheric analyzer CLAM4 from VG Instruments. The angle between sample surface and the electron energy analyzer axis was 60°. Binding energies (BE) were calculated using C 1s peak (284.5 eV) as an internal reference. After subtracting a nonlinear background, each spectrum was resolved into individual component bands of a convoluted Gaussian–Lorentzian (20%) line shape.

## 3. Results and discussion

It has shown that a great amount of precipitated material appears in the bath when mixing the components of the growth solution. The precipitation process diminishes gradually and the growth solution becomes clear. Substrates treated with A or B processes, when introduced into the bath after the initial precipitation process (when the growth solution is clear), do not promote the PbS film growth. The growth of PbS films was observed when the substrates were introduced in the growth solution during the initial stage of the mixing, i.e. when the precipitation process had not finished. On the other hand, the PbS film growth always takes place on a substrate treated with C or D process, probably due to the existence PbS grains on the substrate as a result of the seeding process. It seems that this is a necessary condition to obtain a catalytic surface on the substrate, i.e. the film growth occurs if a catalytic surface is available on the substrate surface. This result agrees with the PbS film deposition described in reference [31].

In order to study the surface composition of the PbS thin films (specially the influence of the growing parameters and the oxidation products at the surface), the samples were analyzed by XPS. From the XPS spectra, the O 1s, S 2p, C 1s and Pb $4f_{7/2}$ BE curves were analyzed. The BE values were taken from reference [32]. In the O 1s region the 529.7–529.9 eV BE was assigned to PbO, 531.3–531.4 eV to $PbCO_3$, 532.6–532.8 eV to $Pb(OH)_2$. Oxygen-containing organic contamination give the O 1s emission at higher BE (533 eV). In Fig. 1, the O 1s BE lines of the XPS spectra of the PbS films are presented. The relative concentrations of the O 1s species are presented in Table 1. The presence of oxygen-containing organic contamination was observed only in the case A as well as the lowest value of the Pb–O bond relative abundance. The solubility product of lead carbonate is very low in comparison to other oxide species [33], thus in the presence of atmospheric $CO_2$ and water vapor or by the influence of the polymers and thiourea from the solution, oxide species present at the surface should be converted to lead carbonate. The oxygen concentration increased from A to D of the Pb–O bond was also observed in the Pb $4f_{7/2}$ BE region (figures are not shown).

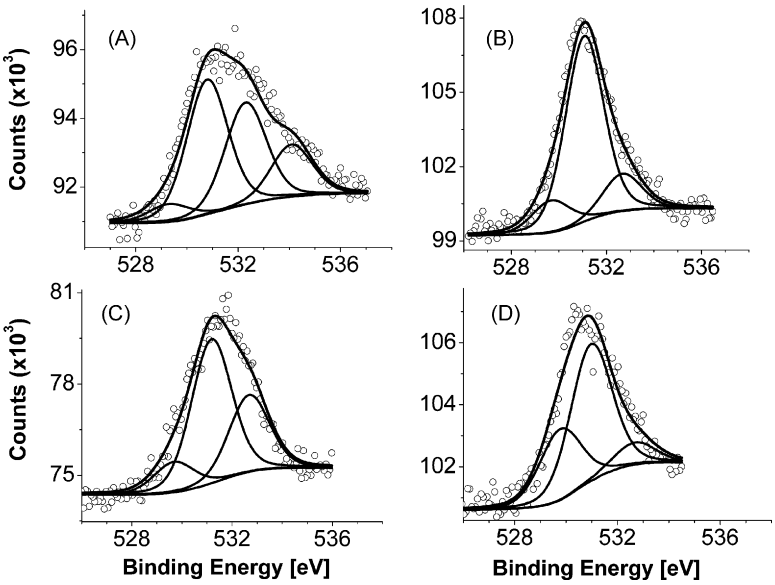


Fig. 1. The curve-fitted O 1s spectra of the PbS analyzed films.

The characteristic RBS spectra of all the analyzed treatments are shown in Fig. 2a. The RBS spectra were analyzed using the RUMP code [27]. To facilitate the RBS spectrum simulation of the PbS multilayer structure films, every single step of the film growth process was analyzed. The spectra of the film/glass interface were simulated considering a linear composition transition from the PbS film to the glass. This consideration roughly corresponds to the known surface glass roughness. The thickness values and the composition of the grown layers were obtained from the RBS spectra simulations (Table 1). Fig. 2b shows the RBS spectrum and a simulation using RUMP code for the case of the treatment D. In all cases, the films showed a constant Pb:S 1:1 stoichiometry throughout the film. The left tail of the Pb signal peaks reveals differences in the film roughness (longer left tail means higher roughness of the films). Samples treated with procedure C have the larger RBS roughness value and those submitted to treatment D the lowest one. We should be aware that the RBS roughness is a combination of the surface roughness and the substrate interface roughness. The RBS roughness of the films was kept dimensionless in the analyses because of the contribution of the film substrate interface.

The thickness and the roughness are parameters that also reveal peculiarities of the deposition process. The film growth onto substrates submitted to the treatments A and B does not take place unless a nucleation layer is created and a catalytic surface of the semiconductor is available. In the cases C and D, the deposition starts once the substrate is introduced into the

Table 1
Relative concentrations of the O 1s species

| Treatment | Oxide, O 1s (PbO) (BE 529.1 eV) | Carbonate, O 1s ($PbCO_3$) (BE 531.1 eV) | OH, O 1s ($Pb(OH)_2$) (BE 532.3 eV) |
|---|---|---|---|
| A | 5.8 | 43.9 | 33.2 |
| B | 12.5 | 72.8 | 14.7 |
| C | 12.12 | 57.3 | 30.6 |
| D | 30.9 | 59.5 | 9.6 |

In the case of A 16.9% of oxygen-containing organic contamination was found (BE above 533 eV). All binding energies values were corrected assuming the BE for C 1s of hydrocarbon type carbon to be 284.5 eV. Values are in percent (%).

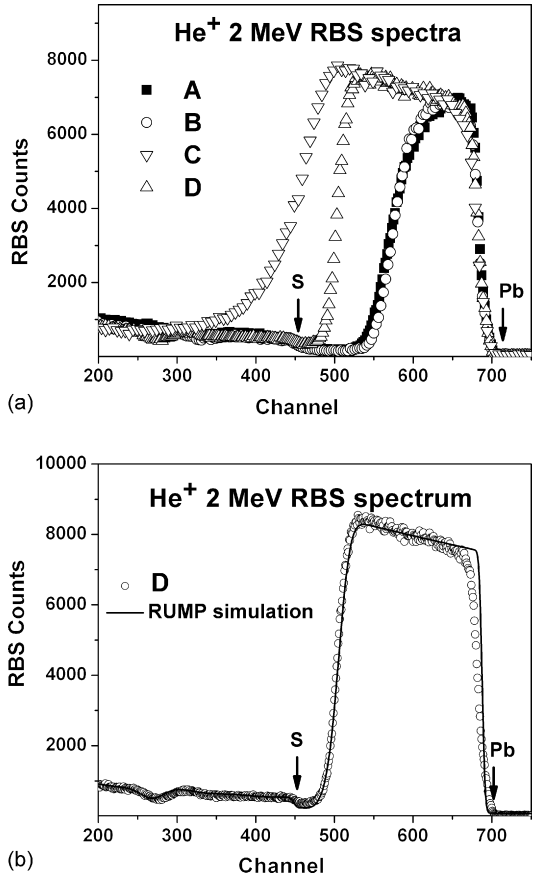


Fig. 2. (a) RBS spectra of the PbS/glass analyzed films and (b) RBS spectra and simulation of the D condition. The arrows indicate the starting position of the Pb and S elements.

Table 2
Thickness (as measured by RBS), mean grain size, roughness, and shape factor for different PbS samples

| Treatment | RBS | AFM | | |
|---|---|---|---|---|
| | Thickness ($10^{15}$ atom/cm$^2$, nm*) | Mean grain size (nm), 10 μm × 10 μm | $R_{ms}$ (nm), 30 μm × 30 μm | SF, 5 μm × 5 μm |
| A | 1650 ± 10, 460 ± 3 | 950 ± 60 | 100 | 0.58 ± 0.01 |
| B | 1650 ± 10, 460 ± 3 | 900 ± 70 | 96 | 0.56 ± 0.02 |
| C | 3500 ± 10, 975 ± 3 | 680 ± 100 | 225 | 0.64 ± 0.02 |
| D | 2650 ± 10, 783 ± 3 | 500 ± 85 | 34 | 0.63 ± 0.01 |

* Thickness values in nm were calculated considering the PbS density values as $3.5885 \times 10^{22}$ atom/cm$^3$.

growth solution. Thus, the beginning of deposition process in the cases A and B is retarded when compared with cases C and D. The growth in the cases A and B is affected by the poor adherence of the PbS grains on the glass substrate. For these reasons, films deposited with the C and D treatments are thicker than those deposited with A and B treatments (Table 2).

From the AFM images (see Fig. 3) the Watershed (WS) patterns were generated to identify the grain boundaries. The way where the grain are arranged in the surface determines whether the grains boundaries are detected by the AFM tip and thus by the WS technique. If two grains of the same height are aligned in such a way that the difference between their boundaries is beyond what the tip can resolve, the two grains will be seen as a single one by the AFM tip and consequently by the WS technique. In our case, the resolution of the AFM tip can be limited laterally by the tip-sample contact area diameter (∼10 nm), which also indicates the smallest distance between grains laterally resolved by the AFM. This value is smaller than the smallest grain measured in the present investigation, so in our measurements this last effect is negligible.

The roughness values, $R_{ms}$, were obtained from the AFM images of 30 μm × 30 μm scans. In the case of the shape factor SF, the analysis corresponds to the 5 μm × 5 μm scans in order to diminish the error of the perimeter identification and to have a relatively good statistics in the number of grains per image (Table 2). A significant difference in the films topography is obtained in dependence of the condition of the initial growth surface. The SF values are roughly close to SF = 0.60, that corresponds to a triangular shape of the grains. This agrees with previously reported PbS crystals obtained using the Langmuir–Blodgett technique [34].

The mean grain size differences among the samples with respect to the influence of the initial stage of the growth surface can be explained in terms of the differences in the growth during the nucleation or induction period. When the substrates are immersed into the growth solution, the first monolayer of

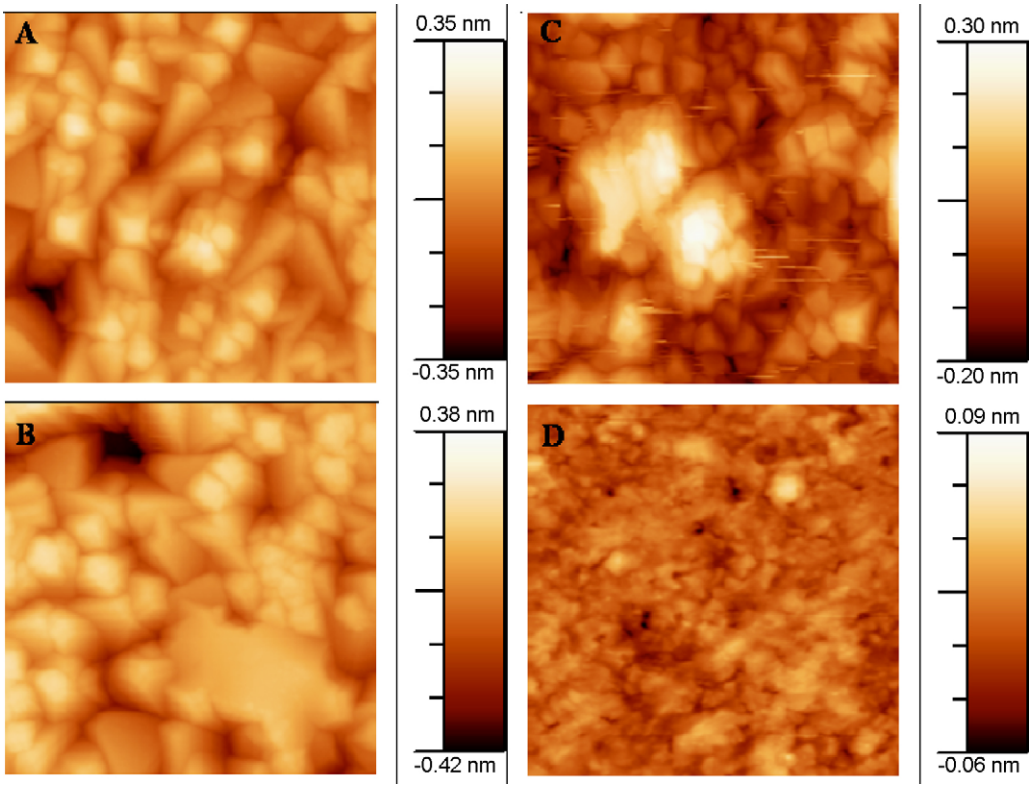


Fig. 3. AFM images of the PbS thin films (5 μm × 5 μm).

PbS is formed from the nucleation centers or PbS seeds grown during the initial precipitation process (treatments A and B) and during the seeding process (treatments C and D). By controlling the surface concentration of seeds, it is possible to control the grain size and the grain size distribution of the final product. If the surface concentration of seeds increases, the maximum size that any one of them may attain will be reduced, and the mean grain size at the end of the process will be smaller [5]. The mean grain size in the case D is smaller than C (Table 2). This fact suggests a higher surface concentration of nucleation centers in sample D as a consequence of a greater stability of the precursor stage. In the case of C, the reduction of nucleation centers, created during the seeding process by the polymer entanglement weakening or dissolution, is faster than in D. Moreover, the amount of effective nucleation centers created during the initial precipitation process is smaller (treatments A and B) than the amount created in the seeding process (treatments C and D), which is confirmed from the mean grain size results (Table 2).

In Fig. 4 are shown the X-ray diffraction pattern obtained from the PbS thin films. The XRD analysis showed a galena type cubic structure for all the samples. In addition, the intensity distribution of the X-ray diffraction peaks deviates from the characteristic distribution of the bulk PbS powders, except in the case A. It can be notice that the intensity of (2 0 0) diffraction peak is much stronger in the other cases (B, C and particularly in case D). This evidences that these polycrystalline thin films of PbS have a preferred orientation with (1 0 0) diffraction planes parallel to the substrate surface.

Fig. 5 shows the relative intensity distribution of the diffraction peaks (in relation to the peaks intensity of the condition A, which was considered as the sample with a random orientation) in regard to (1 0 0) direction. It is easy to observe that the intensity distribution becomes more narrow, with the prevalence of the (1 0 0) direction, in the way as the substrate is coated with colloidal PbS particles in a polyvinyl alcohol solution and then dried. From these results is confirmed that the film texture has a strong influence of the initial conditions of the substrate surface, being more accentuated from A to D treatments. The more oriented film corresponds to the condition D.

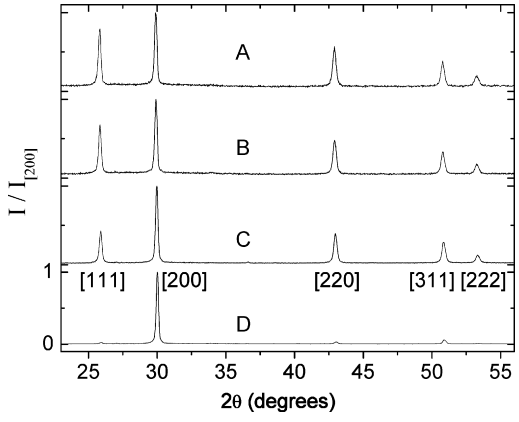


Fig. 4. Normalized X-ray diffraction pattern of PbS thin films with different substrate treatments.

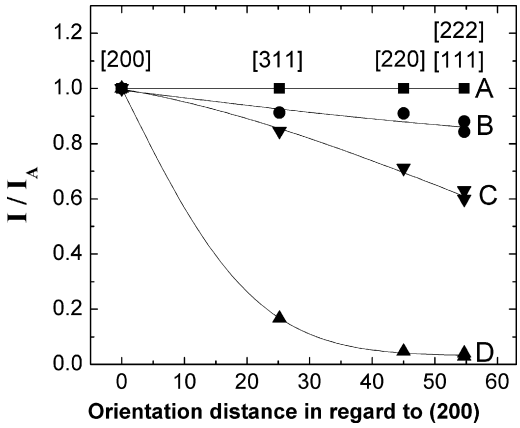


Fig. 5. Film texture analysis of PbS films in regard to (2 0 0) direction.

## 4. Conclusions

Changes in morphology, composition, grain size and thickness were characterized by RBS, XPS, AFM and GIXRD techniques. The PbS films obtained with the inclusion of the polymer showed non-oxygen-containing organic contamination. All samples maintain the Pb:S 1:1 stoichiometry throughout the film. The amount of effective nucleation centers and the mean grain size have being controlled by the substrate colloidal coating. The analysis of the polycrystalline PbS films showed that a preferable (1 0 0) lattice plane orientation parallel to the substrate surface can be obtained using a substrate colloidal coating chemical bath deposition, and the orientation increases when a layer of colloid is initially dried on the substrate. All PbS crystals showed a triangular shape grains.

## Acknowledgments

The authors thank the Latin American Center of Physics (CLAF), and the Brazilian agencies CNPq, CAPES and FAPERJ for the financial support. The authors express their thanks to Prof. M.H.P. Mauricio for the discussion relative to the AFM image analyses.

## References

[1] G.P. Kothiyal, B. Gosh, R.Y. Deshpande, J. Phys. D: Appl. Phys. 13 (1980) 869.
[2] R.H. Bube, Photoelectronic Properties of Semiconductors, Cambridge University Press, 1992, p. 205.
[3] R. Resch, G. Friedbacher, M. Grasserbauer, T. Kannianien, S. Lindros, M. Leskela, L. Niinisto, Appl. Surf. Sci. 120 (1997) 51.
[4] A.A. Preobrajenski, T. Chasse, Appl. Surf. Sci. 142 (1999) 394.
[5] E.M. Larramendi, O. Calzadilla, A. González-Arias, E. Hernández, J. Ruiz-Garcia, Thin Solid Films 389 (2001) 301.
[6] F. Rosei, M. Schunack, P. Jiang, A. Gourdon, E. Laegsgaard, I. Stensgaard, C. Joachim, F. Besenbacher, Science 296 (2002) 328.
[7] T. Yokoyama, S. Yokoyama, T. Kamikado, Y. Okuno, S. Mashiko, Nature 413 (2001) 619.
[8] T.A. Jung, R.R. Schlittler, J.K. Gimzewski, H. Tang, C. Joachim, Science 271 (1996) 181.
[9] T.W. Fishlock, A. Oral, R.G. Egdell, J.B. Pethica, Nature 404 (2000) 743.

[10] Z.J. Donhauser, B.A. Mantooth, K.F. Kelly, 1 L.A. Bumm, J.D. Monnell, J.J. Stapleton, D.W. Price, A.M. Rawlett Jr., D.L. Allara, J.M. Tour, P.S. Weiss, Science 292 (2001) 2303.
[11] S. Datta, W.D. Tian, S.H. Hong, R. Reifenberger, J.I. Henderson, C.P. Kubiak, Phys. Rev. Lett. 79 (1997) 2530.
[12] X.D. Cui, A. Primak, X. Zarate, J. Tomfohr, O.F. Sankey, A.L. Moore, T.A. Moore, D. Gust, G. Harris, S.M. Lindsay, Science 294 (2001) 571.
[13] A.R. Pease, J.O. Jeppesen, J.F. Stoddart, Y. Luo, C.P. Collier, J.R. Heath, Acc. Chem. Res. 34 (2001) 433.
[14] C.P. Collier, E.W. Wong, M. Belohradský, F.M. Raymo, J.F. Stoddart, P.J. Kuekes, R.S. Williams, J.R. Heath, Science 285 (1999) 391.
[15] J. Eastoe, R.A. Cox, Colloids Surf. A: Physicochem. Eng. 101 (1995) 63.
[16] R.S. Kane, R.E. Cohen, R. Silbey, Chem. Mater. 8 (1996) 1919.
[17] M. Mukherjee, A. Datta, D. Chakravorty, Appl. Phys. Lett. 64 (1994) 1159.
[18] X.K. Zhao, S.Q. Xu, J.H. Fendler, Lagmuir 7 (1991) 520.
[19] S. Yang, S. Wang, K.K. Fung, Pure Appl. Chem. 72 (2000) 119.
[20] M. Chen, Y. Xie, Z.Y. Yao, X.M. Liu, Y. Qian, Mater. Chem. Phys. 74 (2002) 109.
[21] J. Wan, X. Chen, Z. Wang, W. Yu, Y. Qian, Mater. Chem. Phys. 88 (2004) 217.
[22] N.M. Huanga, R. Shahidana, P.S. Khiewa, L. Peterb, C.S. Kana, Colloids Surf. A: Physicochem. Eng. 247 (2004) 55.
[23] R.K. Joshia, A. Kanjilalb, H.K. Sehgala, Appl. Surf. Sci. 221 (2004) 43.
[24] N. Wang, K.K. Fung, S. Wang, S. Yang, J. Cryst. Growth 233 (2001) 226.
[25] Z. Zeng, S. Wang, S. Yang, Chem. Mater. 11 (1999) 3365.
[26] S. Wang, S. Yang, Langmuir 16 (2000) 389.
[27] L.R. Doolittle, Nucl. Instrum. Methods B 9 (1985) 344.
[28] J. Serra, Image Analysis and Mahematical Morphology, Academic Press, London, 1988, p. 260.
[29] M. Cremona, M.H.P. Mauricio, L.C. Scavarda do Carmo, R. Prioli, V.B. Nunes, S.I. Zanette, A.O. Caride, M.P. Albuquerque, J. Microsc. 197 (2000) 260.
[30] W. Rasband, National Institute of Health, USA (http://rsb.info.nih.gov/ij).
[31] P.K. Nair, M.T.S. Nair, J. Phys. D 23 (1990) 150.
[32] P. Nowak, K. Laajalehto, I. Kartio, Colloids Surf. A: Physicochem. Eng. 161 (2000) 447.
[33] R. Smith, A. Martell, Critical Stability Constants, Vol. IV: Inorganic Compounds, Plenum Press, New York, 1976, p. 10.
[34] X.K. Zhao, J. Yang, L.D. McCormick, J.H. Fendler, J. Phys. Chem. 96 (1992) 9933.